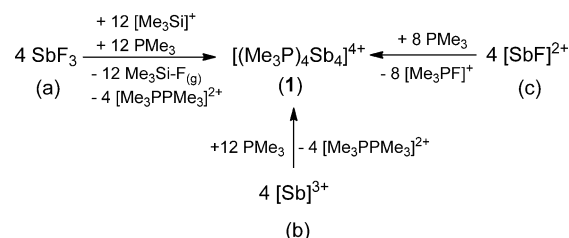


Assembly of a *cyclo*-Tetrastibinotetraphosphonium Tetracation by Reductive Elimination**

Saurabh S. Chitnis, Yuen-Ying Carpenter, Neil Burford, Robert McDonald, and Michael J. Ferguson*

Electron-rich (lone-pair bearing) non-metal elements offer a potentially diverse coordination chemistry as acceptors, and this chemistry is enhanced by the presence of a cationic charge which augments the Lewis acidity at the acceptor site. As such, the coordination chemistry of non-metals offers new synthetic and structural opportunities with guidance from established coordination chemistry of transition metals, and with the possibility of catenation of the nonmetal. For example, the maximally charged Sb^{3+} trication can engage a crown ether^[1] or two 2,2-bipyridine (bipy) ligands.^[2] While phosphine ligands are also expected to support the Sb^{3+} cation, we have discovered that the redox activity between antimony and phosphorus results in formation of an unusual *cyclo*-tetrastibinotetraphosphonium salt.

Addition of three equivalents of trimethylsilyltrifluoromethanesulfonate (TMSOTf) to a suspension of SbF_3 in acetonitrile results in immediate gaseous evolution of Me_3SiF . After the subsequent addition of PMe_3 and heating to reflux for 30 minutes, the ^{31}P , ^1H , and ^{13}C NMR spectra of the clear yellow reaction mixture show quantitative formation of $[\text{Me}_3\text{PPMe}_3][\text{OTf}]_2$ (^{31}P NMR: $\delta = 28.4$ ppm; ^1H NMR: $\delta = 2.39$ ppm; ^{13}C NMR: $\delta = 7.10$ ppm),^[3] and a new compound characterized as $[(\text{Me}_3\text{P})_4\text{Sb}][\text{OTf}]_4$ (**1**) (^{31}P NMR: $\delta = -24.5$ ppm). Identical NMR spectral features are observed for the mixtures of $[\text{bipy}_2\text{Sb}][\text{OTf}]_3$ or $\text{Sb}(\text{OTf})_3$ and PMe_3 in a 1:3 ratio at room temperature. It was not possible to separate **1** from its crystalline mixture with $[\text{Me}_3\text{PPMe}_3][\text{OTf}]_2$. In comparison, mixtures of $[\text{bipy}_2\text{SbF}][\text{OTf}]_2$ or $\text{FSb}(\text{OTf})_2$ and PMe_3 in a 1:2 ratio at 25°C give **1** (^{31}P NMR: $\delta = 148$ ppm; ^{19}F NMR: $\delta = -138$ ppm).^[11] Upon cooling this reaction mixture to -30°C , fractional crystallization affords yellow crystals of **1** ($[\text{OTf}]_4 \cdot 3 \text{CH}_3\text{CN}$).



Scheme 1. Synthesis of **1** from a) SbF_3 , b) $[\text{bipy}_2\text{Sb}]^{3+}$ (or SbOTf_3), and c) $[\text{bipy}_2\text{SbF}]^{2+}$ (or FSbOTf_2).

Formation of $\mathbf{1}[\text{OTf}]_4$ and $[\text{Me}_3\text{PPMe}_3][\text{OTf}]_2$ in the 1:3:3 reaction of SbF_3 with TMSOTf and PMe_3 (Scheme 1 a) can be envisaged as involving the complete abstraction of fluoride anions from SbF_3 by $[\text{Me}_3\text{Si}]^+$, an eight-electron reductive coupling of four Sb^{3+} cations to give $[\text{Sb}_4]^{4+}$ with consequential oxidation of eight PMe_3 molecules to give four $[\text{Me}_3\text{PPMe}_3]^{2+}$ dications, and association of $[\text{Sb}_4]^{4+}$ with four remaining PMe_3 ligands. The mixtures of $[\text{bipy}_2\text{Sb}][\text{OTf}]_3$ or $\text{Sb}(\text{OTf})_3$ with PMe_3 give the same outcome without the requirement of fluoride ion abstraction (Scheme 1 b). By comparison, in the 1:2 reaction of an $[\text{SbF}]^{2+}$ source (e.g. $[\text{bipy}_2\text{SbF}][\text{OTf}]_2$) with PMe_3 (Scheme 1 c), PMe_3 is oxidized to $[\text{Me}_3\text{PF}]^+$. In all cases, PMe_3 behaves coincidentally as a ligand and as a reducing agent.

The solid-state structure of **1**[OTf]₄ has been determined by X-ray crystallography to reveal two ionic formula units in the asymmetric unit, each of which contains a cation composed of a folded Sb₄ square with one PMe₃ attached to each of the antimony centers and four OTf anions. As illustrated in Figure 1, the equatorial configuration of the phosphine substituents allows five Sb...O inter-ion contacts which are nonsymmetrically distributed with one contact to Sb1, two contacts to Sb2, and three contacts to Sb4. While four of the oxygen contacts to the tetracation are peripheral to the Sb₄ framework, a molecule of CH₃CN bridges Sb1 and Sb3 through Sb...N contacts. The Sb–P bond lengths in **1**[OTf]₄ are comparable to those in phosphine complexes of stibonium and stibinidenium cations (range: 2.62–2.56 Å).^[4] Interestingly, the Sb–Sb distances in **1**[OTf]₄ are comparable to those observed in neutral *cyclo-t*Bu₄Sb₄ (**2**) [2.814(2)–2.821(2) Å],^[5] and in rare examples of polyantimony salts, [Me₃SbSbMe₂][A] (A = MeSbBr₃, 2.8205(12) Å,^[6] A = GaCl₄, 2.8278(3) Å^[7]), [Me₂SbSbMe₂SbMe₂][Me₂SbBr₂] (2.8203(4) Å),^[8] [Me₃SbSbMeSbMe₃][GaCl₄]₂ (2.811(1), 2.830(1) Å),^[7] [Me₃SbSbMe₃][SbF₆]₂ (2.7624(11), 2.7867(12) Å),^[9] and [(CyP)₄ClSbSbCl(CyP)₄][AlCl₄]₂ (2.8484(12), 2.8353(12) Å).^[10] The tetracation **1** is related to the recently reported

[*] S. S. Chitnis, Prof. N. Burford
Department of Chemistry, University of Victoria
P.O. Box 3065, Stn. CSC, Victoria, BC (Canada)
E-mail: nburford@uvic.ca

Dr. Y.-Y. Carpenter
Department of Chemistry, Dalhousie University
6274 Coburg Road, PO Box 15000, Halifax, NS (Canada)

Dr. R. McDonald, Dr. M. J. Ferguson
X-Ray Crystallography Lab, University of Alberta
11227 Saskatchewan Drive NW, Edmonton, AB (Canada)

[**] We thank the Natural Sciences and Engineering Council of Canada, and the Vanier Canada Graduate Scholarships Program (SSC) for funding. We thank Dr. Andreas Decken for preliminary X-ray results.

Supporting information for this article is available on the WWW under <http://dx.doi.org/10.1002/anie.201210012>.

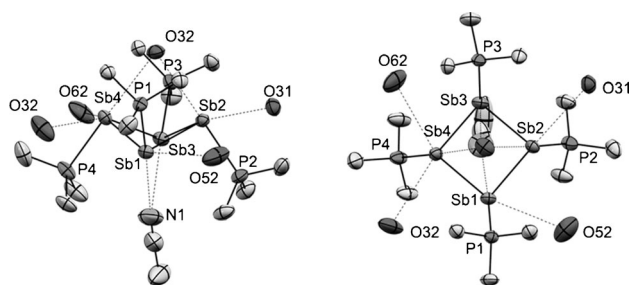
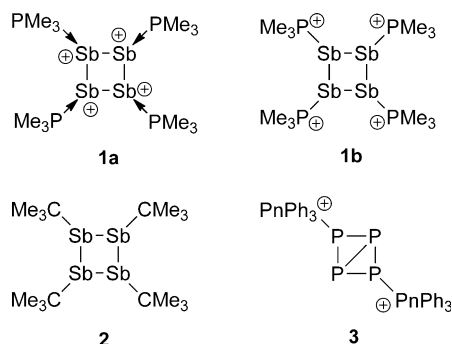


Figure 1. Two views of the cation in $1[\text{OTf}]_4$ in one of the two asymmetric units. Thermal ellipsoids are drawn at 50% probability level. Hydrogen atoms and non-interacting portions of the anions have been omitted for clarity. Experimental/Calculated (gas-phase, $[(\text{Me}_3\text{P})_4\text{Sb}_4]^{4+}$ cation, MP2/6-311g/Def2-TZVPP) bond lengths [Å] and bond angles [°] are as follows: Sb–Sb 2.8411(6)–2.8607(5)/2.853, Sb–P 2.5519(15)–2.5637(16)/2.555, P–C 1.770(7)–1.802(7)/1.795–1.797, Sb–O 3.161–3.316, Sb–N 3.521, $\text{Sb}_n\text{--Sb}_{n+2}$ 3.747–3.780/3.662; Sb–Sb–Sb 82.080(14)–83.088(13)/79.8, Sb–Sb–P 94.10(4)–99.36(4)/97.6.

dications **3** in $[(\text{Ph}_3\text{Pn})_2\text{P}_4][\text{OTf}]_2$ ($\text{Pn} = \text{P}$ or As),^[11] thus illustrating examples of phosphine (or arsine)-stabilized representatives of Pn_4^{4+} and Pn_4^{2+} , respectively.

We have calculated the optimized structure of **1** under anion- and solvent-free conditions in the gas phase and the excellent agreement (Figure 1, caption) between the observed solid-state and calculated gas-phase structures indicates that solvent and anion contacts have negligible influence on the structural features of the tetracation. While **1** can be viewed



as $[\text{Sb}_4]^{4+}$ carrying four phosphine ligands (**1a**), the description as a cyclotetastibine with four exocyclic phosphonium cations (**1b**) is more appropriate based on comparison of the electronic structure with that of its isoelectronic analogue **2**. Figure 2 gives the relative energies and shapes of the eight highest occupied MOs for **1** and the *cyclo*-stibine **2**. As expected, while the orbital energies of **1** are dramatically lower than those of **2** (implying a weak donor ability for **1**, despite the presence of lone pairs at each Sb center), the orbital shapes are remarkably similar, thus highlighting the isolobality of the two species, and are consistent with a single-bonded Sb_4 framework for both. This interpretation is further borne out by the similar Wiberg Bond Index (WBI) calculated for the P–Sb (0.89) and Sb–Sb (0.98) bonds, which are close to single bond values. By comparison, the WBI for the transannular $\text{Sb}_n\text{--Sb}_{n+2}$ (0.02) interaction shows no significant bonding, thus suggesting that the sub-van der Waals transannular interaction is a result rather than the cause of the

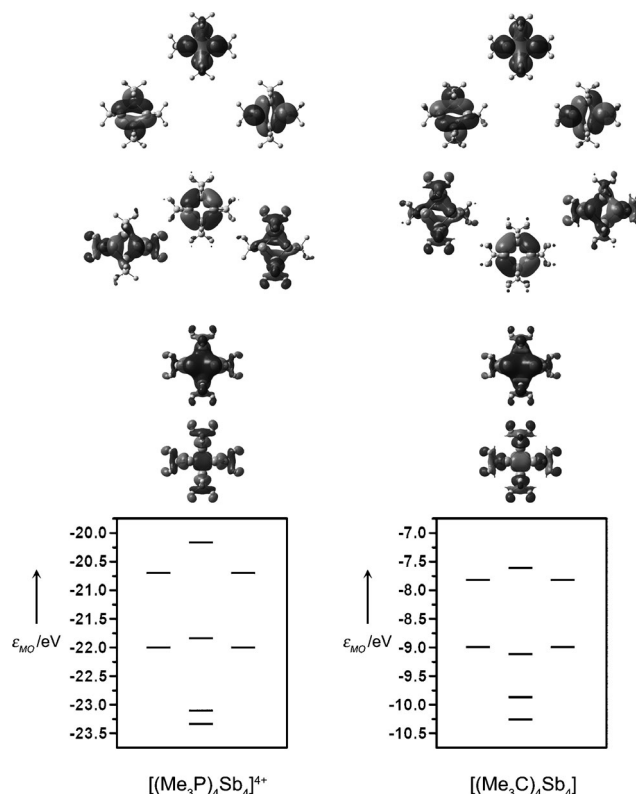


Figure 2. Surface plots (isovalue = 0.02) and energies of the eight highest-energy occupied MOs in the gas-phase structure of cationic **1** (left) and neutral **2** (right) at the MP2/6-311g/Def2-TZVPP level of theory.

observed folded square geometry. The calculated net natural population analysis (NPA) charge for the Sb_4 fragment is only +0.81 *e*, and the remainder of the cationic charge is borne by the four PMe_3 ligands, thus classifying the cation as the cyclotetastibinotetraphosphonium **1b**. Consistently, the P–C bond lengths in **1** (calc.: 1.801 Å, expt.: 1.770(7)–1.802(7) Å) are typical for a trimethylphosphonium fragment (e.g. 1.783(3) Å in the $\text{Me}_3\text{PPMe}_3^{2+}$ dication)^[3] and are significantly shorter than in trimethylphosphine (1.8465(3) Å).^[13]

Solid-state mixtures of $1[\text{OTf}]_4$ and $[\text{Me}_3\text{PPMe}_3][\text{OTf}]_2$ show no decomposition when heated in the dark up to 100 °C under an inert atmosphere for one hour. Heating under dynamic vacuum yields a fine black insoluble powder within minutes, together with $[\text{Me}_3\text{PPMe}_3][\text{OTf}]_2$, thus highlighting the role of the phosphine ligands in stabilizing $1[\text{OTf}]_4$. In contrast to neutral cyclostibines,^[14] solutions of $1[\text{OTf}]_4$ are stable towards equilibrium redistribution into smaller or larger rings. Nevertheless, these solutions react rapidly on ambient exposure to give $[\text{HPMe}_3]^+$, which is evident in the ^{31}P NMR spectra and is interpreted as hydrolysis.

A ^{31}P NMR spectrum of the 1:3:3 mixture of $\text{SbF}_3/\text{TMSOTf}/\text{PMe}_3$ immediately after combination at 25 °C shows five signals including those corresponding to **1** and $[\text{Me}_3\text{PPMe}_3]^{2+}$. A single crystal isolated from this mixture at –35 °C was shown by X-ray crystallography to be a cocrystalline mixture of the stibinotriphosphonium salt $4[\text{OTf}]_3$ and $[\text{Me}_3\text{PPMe}_3][\text{OTf}]_2$, as illustrated in Figure 3. As $4[\text{OTf}]_3$ is

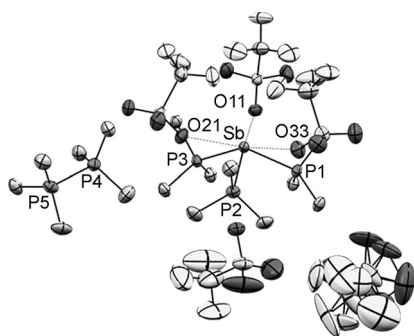


Figure 3. Solid-state structure of $[(\text{Me}_3\text{P})_3\text{Sb}][\text{OTf}]_3$ cocrystallized with $[\text{Me}_3\text{PPMe}_3][\text{OTf}]_2$. Thermal ellipsoids have been drawn at the 50% probability level. Hydrogen atoms have been omitted for clarity. Bond lengths [Å] and angles [°]: Sb–P1 2.6050(7), Sb–P2 2.5974(8), Sb–P3 2.6115(7), Sb–O11 2.960(2), Sb–O21 2.791(2), Sb–O31 2.844(2); P4–P5 2.2235(12); P1–Sb–P2 102.05(3), P2–Sb–P3 11.33(3), P1–Sb–P3 102.40(2), P1–Sb–P2 102.05(3), P1–Sb–P3 102.40(2), P2–Sb–P3 101.33(3).

susceptible to elimination of $[\text{Me}_3\text{PPMe}_3][\text{OTf}]_2$, it has not been possible to obtain $4[\text{OTf}]_3$ as a pure compound. We speculate that **4**, which is formed by $[\text{Me}_3\text{Si}]^+$ -assisted displacement of three fluorides by PMe_3 at Sb, undergoes reductive elimination of $[\text{Me}_3\text{PPMe}_3]^{2+}$ to leave **5**, which sequentially dimerizes to **6**, and then **6** dimerizes to **1** (Scheme 2). The role of **4** as an intermediate is further



Scheme 2. Proposed mechanism for the formation of **1** by reductive elimination of diphosphonium from a stibinotriphosphonium cation (**4**).

supported by the observation that 1:3 mixtures of preformed $\text{Sb}(\text{OTf})_3$ with PMe_3 or $[\text{bipy}_2\text{Sb}][\text{OTf}]_3$ with PMe_3 (Scheme 1b) also yield $1[\text{OTf}]_4$ and $[\text{Me}_3\text{PPMe}_3][\text{OTf}]_2$, thereby precluding the role of fluoroantimony cations as intermediates.

Reductive elimination of diphosphonium dications from metal phosphine complexes has been proposed previously as the mechanism responsible for the observation of $[\text{Me}_3\text{PPMe}_3]^{2+}$ from the decomposition of trimethylphosphine complexes of Cu^{II} and Ti^{III} , which also yields the corresponding reduced Cu^{I} and Ti^{I} species.^[15] Moreover, the dimerization of an in situ generated neutral stibinidene (RSb) to give an isolable distibene ($\text{RSb}=\text{SbR}$) has been observed previously,^[16] and we expect the cationic stibinidene derivative postulated here ($[\text{Me}_3\text{PSb}]^+$) to be even more reactive towards dimerization because of its enhanced electrophilicity.

In contrast, a different redox pathway to $1[\text{OTf}]_4$, one that does involve fluoroantimony intermediates, is clearly implicated in the room temperature reaction between two equivalents of PMe_3 and $[\text{bipy}_2\text{SbF}][\text{OTf}]_2$ or FSbOTf_2 , and yields eight equivalents of free bipy and eight equivalents of $[\text{Me}_3\text{PF}][\text{OTf}]$ as the oxidation product (Scheme 1c). We

speculate that the in situ formation of $[(\text{bipy})_n(\text{PMe}_3)_2\text{SbF}]^{2+}$ is followed by reductive elimination of $[\text{Me}_3\text{PF}]^+$ to yield **5**, which assembles to give **1**. Examples of metal complexes undergoing reductive elimination of halophosphonium cations are limited to the elimination of $[\text{Me}_3\text{PI}]^+$ from heteroleptic PMe_3 complexes of Fe^{II} or W^{V} metals, which also yield the corresponding Fe^0 and W^{III} complexes as the reduction products.^[17] To the best of our knowledge, no such examples have been reported for antimony complexes.

In summary, a *cyclo*-tetrastibinotetraphosphonium tetracation is formed in the reaction of stibine cations with PMe_3 to give coordination complexes which undergo reductive elimination of diphosphonium or fluorophosphonium cations to effect coupling of antimony centers. The observations reveal new redox chemistry for antimony that relates to transition-metal coordination chemistry and new approaches to both P–P and Sb–Sb catenation.

Experimental Section

1 $[\text{OTf}]_4$: SbF_3 (1 mmol, 0.179 g) and TMSOTf (2 mmol, 0.444 g) were stirred in CH_3CN (4 mL) for 16 h. Me_3SiF and the solvent was removed under vacuum and the white powder (FSbOTf_2) was washed with *n*-pentane (4 mL) and dried under vacuum. A solution of PMe_3 (2 mmol, 0.152 g) in CH_3CN (3 mL) was added dropwise to the stirred powder. The resulting clear yellow solution was stirred for 0.25 h, concentrated under vacuum, and placed in the freezer (-30°C) overnight to yield yellow crystals of **1** $[\text{OTf}]_4 \cdot 3\text{CH}_3\text{CN}$. The crystals were isolated by pipetting off the supernatant and washed with 0.5 mL cold (-30°C) CH_3CN . Recrystallization from CH_3CN and removal of coordinated solvent under vacuum (5×10^{-2} mbar) at 25°C gave analytically pure **1** $[\text{OTf}]_4$ as a fine yellow powder. Yield: 0.153 g, 44%. $\text{C}_2\text{H}_4\text{N}$ analysis (%): calcd./found for $\text{C}_{16}\text{H}_{36}\text{O}_{12}\text{F}_{12}\text{S}_4\text{P}_4\text{Sb}_4$: C 13.85/13.52, H 2.61/2.58, N 0.00/<0.03 (limit of detection). M.p.: 116°C (dec.). Crystal data for **1** $[\text{OTf}]_4 \cdot 3\text{CH}_3\text{CN}$: $\text{C}_{22}\text{H}_{45}\text{F}_{12}\text{N}_3\text{O}_{12}\text{P}_4\text{S}_4\text{Sb}_4$, size $0.39 \times 0.33 \times 0.10 \text{ mm}^3$, monoclinic, $P2_1$ (No. 4), $a = 12.8449(6)$, $b = 21.7755(9)$, $c = 18.1186(8) \text{ Å}$, $\beta = 96.9476(6)^\circ$, $V = 5030.6(4) \text{ Å}^3$, $z = 4$, $\mu = 2.512 \text{ mm}^{-1}$, $2\theta_{\text{max}} = 55.10^\circ$, collected (independent) reflection = 45011 (23046), 1038 parameters, $R1 = 0.0322$, $wR2 = 0.0787$ for all data, max/min residual electron density = $0.917/-0.763 \text{ e Å}^{-3}$.

Crystal data for $[(\text{Me}_3\text{P})_3\text{Sb}][\text{Me}_3\text{PPMe}_3][\text{OTf}]_5 \cdot \text{CH}_3\text{CN}$: $\text{C}_{22}\text{H}_{48}\text{F}_{15}\text{N}_3\text{O}_{15}\text{P}_5\text{S}_5\text{Sb}$, size $0.39 \times 0.24 \times 0.22 \text{ mm}^3$, monoclinic, $P2_1/n$ (an alternate setting of $P2_1/c$ (No.14)), $a = 17.8657(4)$, $b = 11.5090(3)$, $c = 25.2577(6) \text{ Å}$, $\beta = 99.0800(10)^\circ$, $V = 5128.3(2) \text{ Å}^3$, $z = 4$, $\mu = 8.655 \text{ mm}^{-1}$, $2\theta_{\text{max}} = 136.09^\circ$, collected (independent) reflections = 31843 (9429), 651 parameters, $R1 = 0.0367$, $wR2 = 0.0961$ for all data, max/min residual electron density = $1.161/-1.221 \text{ e Å}^{-3}$.

CCDC 914945 ($[(\text{Me}_3\text{P})_3\text{Sb}][\text{Me}_3\text{PPMe}_3][\text{OTf}]_5 \cdot \text{CH}_3\text{CN}$) and 914946 (**1** $[\text{OTf}]_4 \cdot 3\text{CH}_3\text{CN}$) contains the supplementary crystallographic data for this paper. These data can be obtained free of charge from The Cambridge Crystallographic Data Centre via www.ccdc.cam.ac.uk/data_request/cif.

For spectroscopic details, see the Supporting Information.

Received: December 14, 2012

Revised: February 2, 2013

Published online: March 26, 2013

Keywords: antimony · cations · coordination modes · phosphorus · solid-state structures

-
- [1] R. Garbe, B. Vollmer, B. Neumüller, J. Pebler, K. Dehnicke, *Z. Anorg. Allg. Chem.* **1993**, 619, 271–276.
- [2] S. S. Chitnis, N. Burford, M. J. Ferguson, *Angew. Chem.* **2013**, 125, 2096–2099; *Angew. Chem. Int. Ed.* **2013**, 52, 2042–2045.
- [3] J. J. Weigand, S. D. Riegel, N. Burford, A. Decken, *J. Am. Chem. Soc.* **2007**, 129, 7969–7976.
- [4] S. S. Chitnis, B. Peters, E. Conrad, N. Burford, R. McDonald, M. J. Ferguson, *Chem. Commun.* **2011**, 47, 12331–12333.
- [5] O. Mundt, G. Becker, H. J. Wessely, H. J. Breunig, H. Z. Kischkel, *Z. Anorg. Allg. Chem.* **1982**, 486, 70–89.
- [6] A. Althaus, H. J. Breunig, E. Lork, *Chem. Commun.* **1999**, 1971–1972.
- [7] C. Hering, M. Lehmann, A. Schulz, A. Villinger, *Inorg. Chem.* **2012**, 51, 8212–8224.
- [8] H. J. Breunig, M. Denker, E. Lork, *Angew. Chem.* **1996**, 108, 1081–1082; *Angew. Chem. Int. Ed. Engl.* **1996**, 35, 1005–1006.
- [9] R. Minkwitz, C. Hirsch, *Z. Anorg. Allg. Chem.* **1999**, 625, 1674–1682.
- [10] E. Conrad, N. Burford, U. Werner-Zwanziger, R. McDonald, M. J. Ferguson, *Chem. Commun.* **2010**, 46, 2465–2467.
- [11] M. Donath, E. Conrad, P. Jerabek, G. Frenking, R. Frohlich, N. Burford, J. J. Weigand, *Angew. Chem.* **2012**, 124, 3018–3021; *Angew. Chem. Int. Ed.* **2012**, 51, 2964–2967.
- [12] A. M. Forster, A. J. Downs, *Polyhedron* **1985**, 4, 1625–1635.
- [13] L. S. Bartell, L. O. Brockway, *J. Chem. Phys.* **1960**, 32, 512–515.
- [14] H. J. Breunig, K. H. Ebert, S. Gulec, J. Probst, *Chem. Ber.* **1995**, 128, 599–603.
- [15] R. M. Siddique, J. M. Winfield, *Can. J. Chem.* **1989**, 67, 1780–1784.
- [16] T. Sasamori, Y. Arai, N. Takeda, R. Okazaki, N. Tokitoh, *Chem. Lett.* **2001**, 42–43.
- [17] Fe: G. Bellachioma, G. Cardaci, A. Macchioni, C. Venturi, C. Zuccaccia, *J. Organomet. Chem.* **2006**, 691, 3881–3888; W: A. L. Filippou, E. O. Fischer, H. G. Alt, *J. Organomet. Chem.* **1988**, 344, 215.
-